

# Technical Note on CERES EBAF Ed2.6r

## TOA Outgoing Shortwave Radiation (rsut)

### 1. Intent of This Document and POC

**1a)** This document is intended for users who wish to compare satellite derived observations with climate model output in the context of the CMIP5/IPCC historical experiments. Users are not expected to be experts in satellite derived Earth system observational data. This document summarizes essential information needed for comparing this dataset to climate model output. References are provided at the end of this document to additional information.

This NASA dataset is provided as part of an experimental activity to increase the usability of NASA satellite observational data for the modeling and model analysis communities. This is not a standard NASA satellite instrument product, but does represent an effort on behalf of data experts to identify a product that is appropriate for routine model evaluation. The data may have been reprocessed, reformatted, or created solely for comparisons with climate model output. Community feedback to improve and validate the dataset for modeling usage is appreciated. Email comments to [HQ-CLIMATE-OBS@mail.nasa.gov](mailto:HQ-CLIMATE-OBS@mail.nasa.gov).

Dataset File Name (as it appears on the ESG):

rsut\_CERES-EBAF\_L4\_Ed2-6r\_200003-201106.nc

**1b)** Technical point of contact for this dataset:

Norman Loeb email: [Norman.g.loeb@nasa.gov](mailto:Norman.g.loeb@nasa.gov)

### 2. Data Field Description

CF variable name, units:	TOA Outgoing Shortwave Radiation (rsut), $\text{Wm}^{-2}$
Spatial resolution:	1°x1° latitude by longitude
Temporal resolution and extent:	Monthly averaged from 03/2000 to 06/2011
Coverage:	Global

### 3. Data Origin

CERES instruments fly on the Terra (descending sun-synchronous orbit with an equator crossing time of 10:30 A.M. local time) and Aqua (ascending sun-synchronous orbit with an equator crossing time of 1:30 P.M. local time) satellites. Each CERES instrument measures filtered radiances in the shortwave (SW; wavelengths between 0.3 and 5  $\mu\text{m}$ ), total (TOT; wavelengths between 0.3 and 200  $\mu\text{m}$ ), and window (WN; wavelengths between 8 and 12  $\mu\text{m}$ ) regions. To correct for the imperfect spectral response of the instrument, the filtered radiances are converted to unfiltered reflected solar, unfiltered emitted terrestrial longwave (LW) and window (WN) radiances (Loeb et al. 2001). Since there is no LW channel on CERES, LW daytime radiances are determined from the difference between the TOT and SW channel radiances. Instantaneous top-of-atmosphere (TOA) radiative fluxes are estimated from unfiltered radiances using empirical angular distribution models (ADMs; Loeb et al. 2003, 2005) for scene types identified using retrievals from Moderate Resolution Imaging Spectrometer (MODIS) measurements

(Minnis et al. 2011). Monthly mean fluxes are determined by spatially averaging the instantaneous values on a  $1^\circ \times 1^\circ$  grid, temporally interpolating between observed values at 1-h increments for each hour of every month, and then averaging all hour boxes in a month. Level-3 processing is performed on a nested grid, which uses  $1^\circ$  equal-angle regions between  $45^\circ\text{N}$  and  $45^\circ\text{S}$ , and maintains area consistency at higher latitudes. The fluxes are then output to a complete  $360 \times 180$   $1^\circ \times 1^\circ$  grid created by replication.

Monthly regional CERES SW TOA fluxes in the CMIP5 archive are from the CERES Energy Balanced and Filled (EBAF) Ed2.6r data product. This version differs from EBAF Ed1.0 (Loeb et al., 2009) in many respects. SW TOA fluxes in EBAF Ed2.6r are derived from two standard gridded daily CERES products that utilize complementary time interpolation methods:

- (i) SSF1deg\_Ed2.6: SW radiative fluxes between CERES observation times are determined from the observed fluxes by using scene-dependent diurnal albedo models to estimate how TOA albedo (and therefore flux) changes with solar zenith angle for each local time, assuming the scene properties remain invariant throughout the day. The sun angle-dependent diurnal albedo models are based upon the CERES ADMs developed for the Tropical Rainfall Measuring Mission (TRMM) satellite (Loeb et al. 2003).
- (ii) SYN1deg\_Ed2.6: SW radiative fluxes between CERES observation times are determined by supplementing the CERES observations with 3-hourly TOA fluxes derived from 5 geostationary satellites. Doelling et al. (2012) provides a detailed description of how broadband TOA fluxes are derived from geostationary data.

SSF1deg provides global coverage daily with excellent calibration stability, but samples only at specific times of the day due to the sun-synchronous orbit. While the SYN1deg approach provides improved diurnal coverage by merging CERES and 3-hourly geostationary data, artifacts in the GEO data over certain regions and time periods can introduce larger uncertainties. In order to remove most of the GEO derived flux biases, the fluxes are normalized at Terra or Aqua observation times to remain consistent with the CERES instrument calibration (Doelling et al., 2011). Nevertheless, spurious jumps in the SW TOA flux record can still occur when GEO satellites are replaced due to changes in satellite position, calibration and/or visible sensor spectral response, and imaging schedules. Such artifacts in the GEO data can be problematic in studies of TOA radiation interannual variability and/or trends.

To maintain the excellent CERES instrument calibration stability of SSF1deg and also preserve diurnal information in SYN1deg, EBAF Ed2.6r uses a new approach involving scene dependent diurnal corrections to convert daily regional mean SSF1deg fluxes to diurnally complete values analogous to SYN1deg, but without geostationary artifacts. The diurnal corrections are ratios of SYN1deg-to-SSF1deg fluxes defined for each of the five geostationary satellite domains for each calendar month. They depend upon surface type and MODIS cloud fraction and height retrievals, and thus can vary from one day to the next along with the cloud properties (i.e., they are dynamic). For March 2000-June 2002, TOA fluxes are based upon CERES observations from the Terra spacecraft, while for July 2002 onwards, CERES observations from both Terra and Aqua are utilized in order to improve the accuracy of the diurnal corrections. In EBAF Ed1.0 and EBAF Ed2.5, only Terra data were used and the main input was either CERES SRBAVG GEO Edition2D or CERES SYN Ed2.5, which both explicitly rely on GEO for time interpolation. An assessment of this new approach for EBAF Ed2.6r is provided in Section 4.

As in previous versions of EBAF (Loeb et al., 2009), the CERES SW and LW fluxes in EBAF Ed2.6r are adjusted within their range of uncertainty to remove the inconsistency between average global net TOA flux and heat storage in the earth-atmosphere system, as determined primarily from ocean heat content anomaly (OHCA) data. In the current version, described in Loeb et al. (2012a), the global annual mean values are adjusted such that the July 2005–June 2010 mean net TOA flux is  $0.58 \pm 0.38 \text{ Wm}^{-2}$  (uncertainties at the 90% confidence level). The uptake of heat by the Earth for this period is estimated from the sum of: (i)  $0.47 \pm 0.38 \text{ Wm}^{-2}$  from the slope of weighted linear least square fit to ARGO OHCA data (Roemmich et al., 2009) to a depth of 1800 m analyzed following Lyman and Johnson (2008); (ii)  $0.07 \pm 0.05 \text{ Wm}^{-2}$  from ocean heat storage at depths below 2000 m using data from 1981–2010 (Purkey and Johnson, 2010), and (iii)  $0.04 \pm 0.02 \text{ Wm}^{-2}$  from ice warming and melt, and atmospheric and lithospheric warming (Hansen et al., 2005; Trenberth, 2009). This results in a net flux balance of  $0.58 \text{ Wm}^{-2}$  for the CERES 10-year record.

#### 4. Validation and Uncertainty Estimate

Regional monthly mean SW TOA fluxes are derived from Level-1 and -2 data. The Level-1 data correspond to calibrated radiances. Here we use the latest CERES gains and time-dependent spectral response function values (Thomas et al., 2010, Loeb et al., 2012b). The Level-2 TOA fluxes are instantaneous values at the CERES footprint scale. Their accuracy has been evaluated in several articles (Loeb et al., 2006; Loeb et al., 2007; Kato and Loeb, 2005). The SSF1deg and SYN1deg product used is evaluated in Loeb et al. (2012b) and Doelling et al. (2012).

Figs. 1a and 1b provide regional plots of mean SW TOA flux and interannual variability for the month of March based upon all March months between 2000 and 2010. The regional  $1^\circ \times 1^\circ$  standard deviation ranges from near zero at the poles to  $40 \text{ Wm}^{-2}$  in the western tropical Pacific Ocean region. Considering all  $1^\circ \times 1^\circ$  regions, the overall global regional standard deviation in SW TOA flux is  $22 \text{ Wm}^{-2}$ , and the overall global mean SW TOA flux is  $99.7 \text{ Wm}^{-2}$ .

The uncertainty in  $1^\circ \times 1^\circ$  regional SW TOA flux is evaluated separately for 03/2000–06/2002 (Terra-Only period) and for 07/2002–12/2010 (Terra-Aqua period). To determine uncertainties for the Terra-Only period, we use data from the Terra-Aqua period and compare regional fluxes derived by applying diurnal corrections to the Terra SSF1deg product with regional fluxes determined by averaging fluxes from the Terra and Aqua SYN1deg Ed2.6 data products. The SYN1deg Ed2.6 products combine CERES observations on Terra or Aqua with five geostationary instruments covering all longitudes between  $60^\circ\text{S}$  and  $60^\circ\text{N}$ , thus providing the most temporally and spatially complete CERES dataset for Terra or Aqua. Figs. 2a and 2b show maps of the regional bias and RMS error. The overall regional RMS error is  $4 \text{ Wm}^{-2}$ . In stratocumulus regions, RMS differences are typically around  $5 \text{ Wm}^{-2}$ , or approximately 5% of the regional mean value.

Uncertainties for the Terra-Aqua period are determined by comparing regional fluxes derived by applying diurnal corrections to the average of Terra and Aqua SSF1deg Ed2.6 fluxes with average Terra and Aqua regional fluxes from SYN1deg Ed2.6. Results, shown in Fig. 3a and 3b, show much improvement over the Terra-only case in Fig. 2, with regional errors decreasing to  $2.7 \text{ Wm}^{-2}$  overall, and errors  $< 3 \text{ Wm}^{-2}$  in stratocumulus regions.

To place the above results into context, regional mean and RMS differences between Terra and Aqua SYN1deg Ed2.6 SW TOA fluxes are provided in Fig. 4a and 4b. Overall, the RMS

difference is  $4.4 \text{ Wm}^{-2}$ . RMS differences  $>10 \text{ Wm}^{-2}$  are evident over Africa, Tibet and over isolated regions in the Americas. Since the same geostationary data are used for both Terra and Aqua SYN1deg products, why should there be any discrepancy? The regional discrepancies are mainly associated with the regional normalization of 3-hourly geostationary data to either Terra or Aqua anchor measurements can have a time mismatch of up to 1.5 hours, causing cloud conditions and fluxes to differ (Doelling et al., 2011). Consequently, a longitudinal striping pattern appears that is correlated with the time separation between the geostationary and sun-synchronous observations.

If we assume the overall uncertainty is due to the EBAF diurnal correction, the combined sum of the Terra and Aqua SYN1deg Ed2.6 SW regional fluxes, which is given by the RMS difference between Terra and Aqua SYN1deg divided by the square root of 2, and CERES instrument calibration uncertainty of  $1 \text{ Wm}^{-2}$  ( $1\sigma$ ), the regional uncertainty for EBAF Ed2.6r for March 2000–June 2002 is  $\sqrt{4^2 + (4.4/2)^2 + 1^2}$  or approximately  $5 \text{ Wm}^{-2}$ , and for July 2002–December 2010 is  $\sqrt{2.7^2 + (4.4/2)^2 + 1^2}$  or  $4 \text{ Wm}^{-2}$ .

While the diurnal corrections applied to SSF1deg Ed2.6 fluxes do introduce a slight increase regional SW TOA flux uncertainty, they dramatically improve the EBAF record by minimizing the impact of geostationary satellite artifacts, especially with respect to temporal regional trends. As an example, Fig. 5a and 5b show regional trends in SW TOA flux for from EBAF Ed2.6r and SYN Ed2.6 for March 2000–December 2010. In Fig. 5b, vertical lines corresponding to geostationary satellite boundaries are clearly visible around  $30^\circ\text{E}$ ,  $100^\circ\text{E}$ ,  $180^\circ\text{E}$ ,  $105^\circ\text{W}$  and  $40^\circ\text{W}$ . The geostationary artifacts are more pronounced over Africa and Asia, but also show up to the east of South America. In contrast, the geostationary artifacts are largely absent in Fig. 5a, which is based upon EBAF Ed2.6r data. Figs. 6a and 6b provide SW TOA flux anomaly differences between SYN1deg and SSF1deg Ed2.6 as well as EBAF and SSF1deg Ed2.6 for  $60^\circ\text{S}$ – $60^\circ\text{N}$  (Fig. 6a) and the same latitude range but restricted to  $101.5^\circ\text{E}$ – $140^\circ\text{E}$  (Fig. 6b). The latter region covers much of the Western Tropical Pacific Ocean region, Indonesia, and East Asia. In both cases, the SYN1deg Ed2.6 results show a sharp decline relative to SSF1deg Ed2.6 reaching  $0.4 \text{ Wm}^{-2}$  per decade for  $60^\circ\text{S}$ – $60^\circ\text{N}$  and  $1.8 \text{ Wm}^{-2}$  per decade in the smaller region. In both case, the new EBAF2.5B results remain well within  $0.1 \text{ Wm}^{-2}$  per decade of SSF1deg Ed2.6, while accounting for the diurnal cycle.

Table 1 compares global TOA averages for EBAF Ed2.6r with earlier versions EBAF Ed1.0, EBAF Ed2.5 and EBAF Ed2.6. All-sky SW TOA flux in Ed2.6r is  $0.5 \text{ Wm}^{-2}$  greater than Ed1.0 and  $0.3$ – $0.4 \text{ Wm}^{-2}$  greater than Ed2.5. The main difference between all-sky SW TOA fluxes in EBAF Ed2.6r and Ed2.5 is that Ed2.6r uses the methodology described in Section 3, while EBAF Ed2.5 is derived from SYN1deg-lite Ed2.5, which relies explicitly on geostationary satellite measurements to complete the diurnal cycle. Another difference that applies to all TOA flux variables is that EBAF Ed2.6r applies geodetic weighting when averaging globally, while geocentric weighting is assumed in EBAF Ed2.5 and EBAF Ed1.0.

Table 1 Global mean TOA fluxes from EBAF Ed1.0, EBAF Ed2.5, EBAF Ed2.6 and EBAF 2.6r for March 2000–February 2005 and March 2000–February 2010.

	<b>March 2000–February 2005</b>			
	<b>EBAF Ed1.0</b>	<b>EBAF Ed2.5</b>	<b>EBAF Ed2.6</b>	<b>EBAF Ed2.6r</b>
Incoming Solar	340.0	340.2	340.5	340.0
LW (all-sky)	239.6	239.6	239.9	239.7
SW (all-sky)	99.5	99.7	100.0	99.8
Net (all-sky)	0.85	0.85	0.55	0.54
LW (clear-sky)	269.1	266.2	266.5	266
SW (clear-sky)	52.9	52.4	52.6	52.5
Net (clear-sky)	18.0	21.5	21.4	21.5
	<b>March 2000–February 2010</b>			
	<b>EBAF Ed1.0</b>	<b>EBAF Ed2.5</b>	<b>EBAF Ed2.6</b>	<b>EBAF Ed2.6r</b>
Incoming Solar		340.1	340.4	339.9
LW (all-sky)		239.6	239.9	239.6
SW (all-sky)		99.5	99.9	99.7
Net (all-sky)		1.0	0.59	0.57
LW (clear-sky)		266.0	266.4	265.9
SW (clear-sky)		52.4	52.5	52.5
Net (clear-sky)		21.6	21.5	21.5

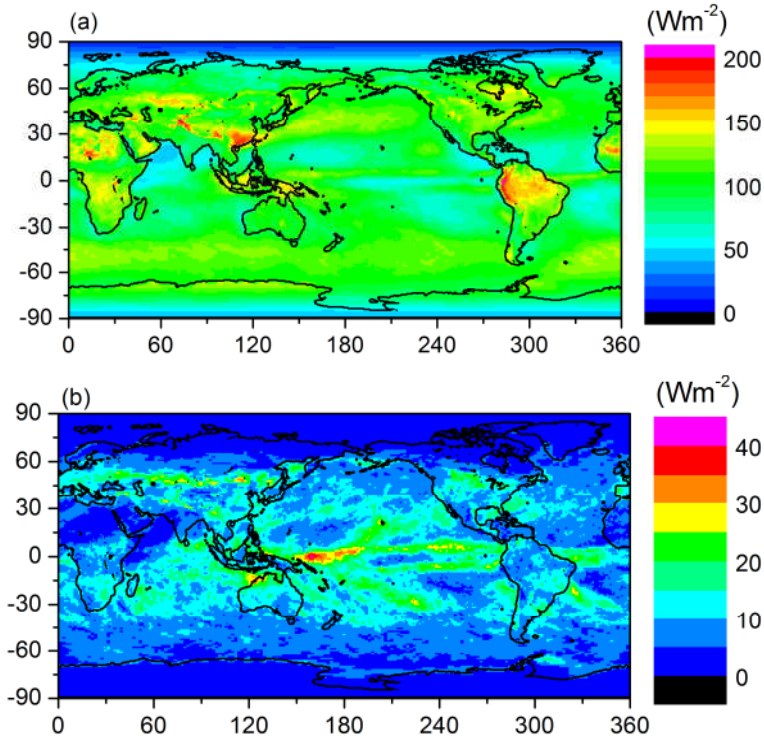


Figure 1 (a) Average and (b) standard deviation of SW TOA flux determined from all March months from 2000–2010 using the CERES EBAF Ed2.6r product.

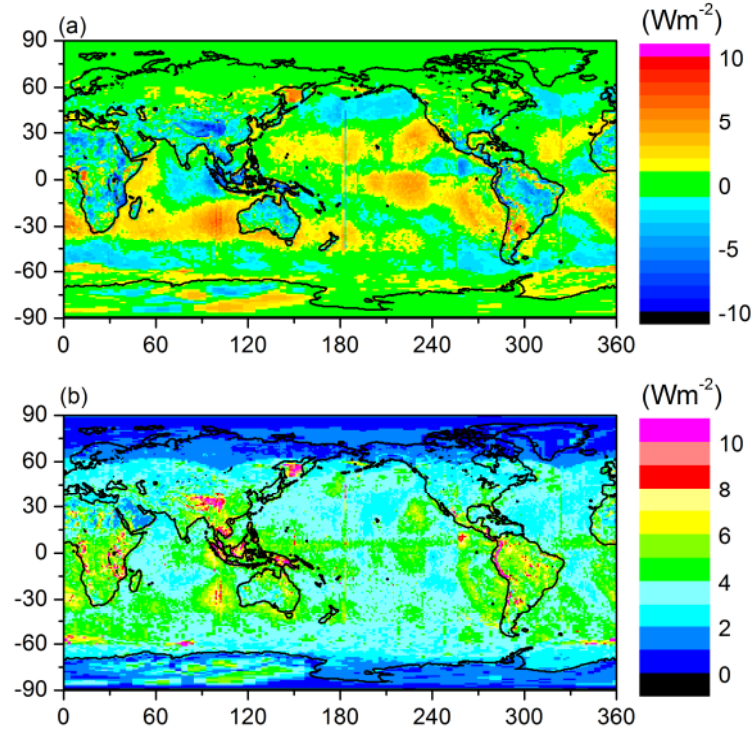


Figure 2 (a) Bias and (b) RMS difference between fluxes derived by applying diurnal corrections to Terra SSF1deg Ed2.6 and TOA fluxes from the average of Terra and Aqua SYN1deg.

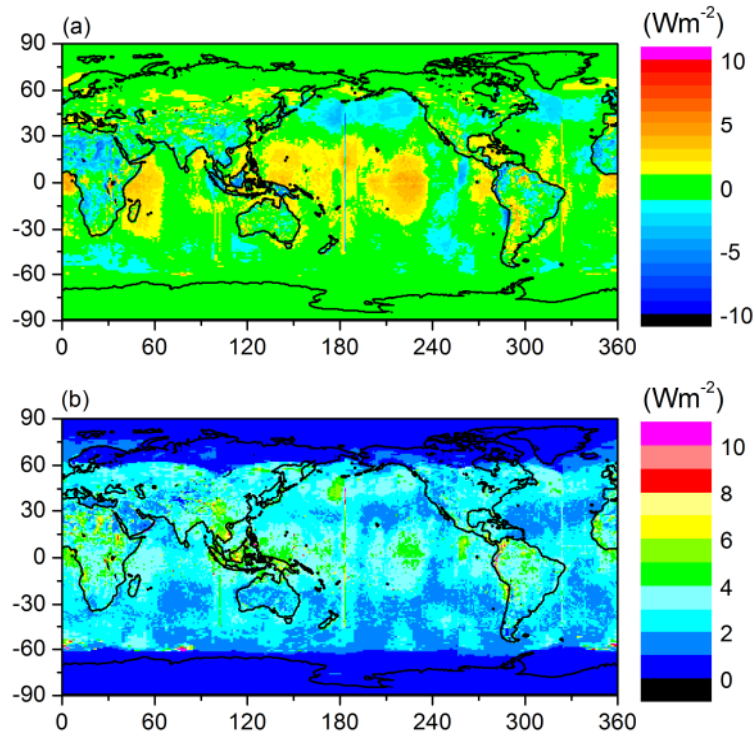


Figure 3 Same as Fig.2 but after applying diurnal corrections to combined Terra+Aqua SSF1deg Ed2.6 fluxes.

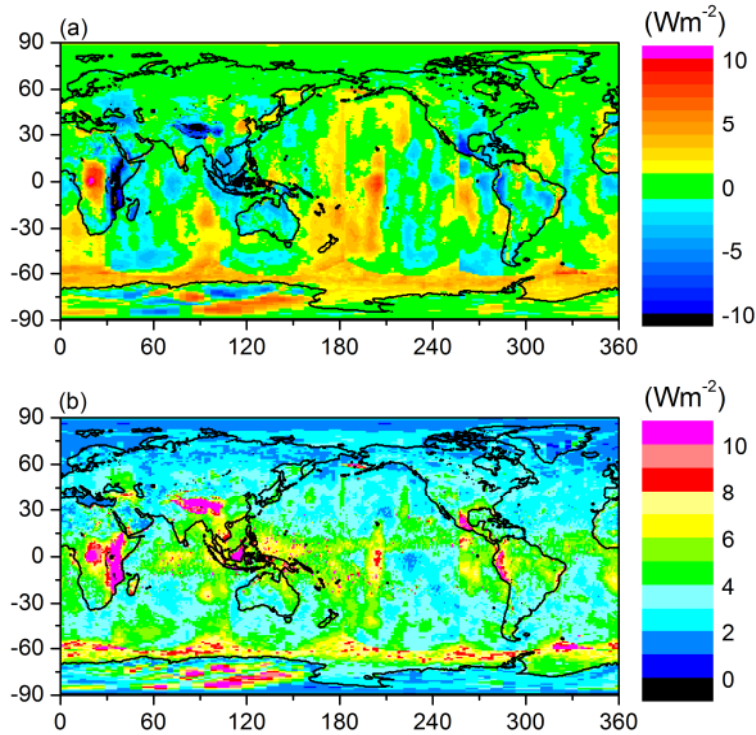


Figure 4 (a) Mean and (b) RMS difference between SW TOA fluxes from CERES Terra and CERES Aqua SYN1deg Ed2.6 data products.



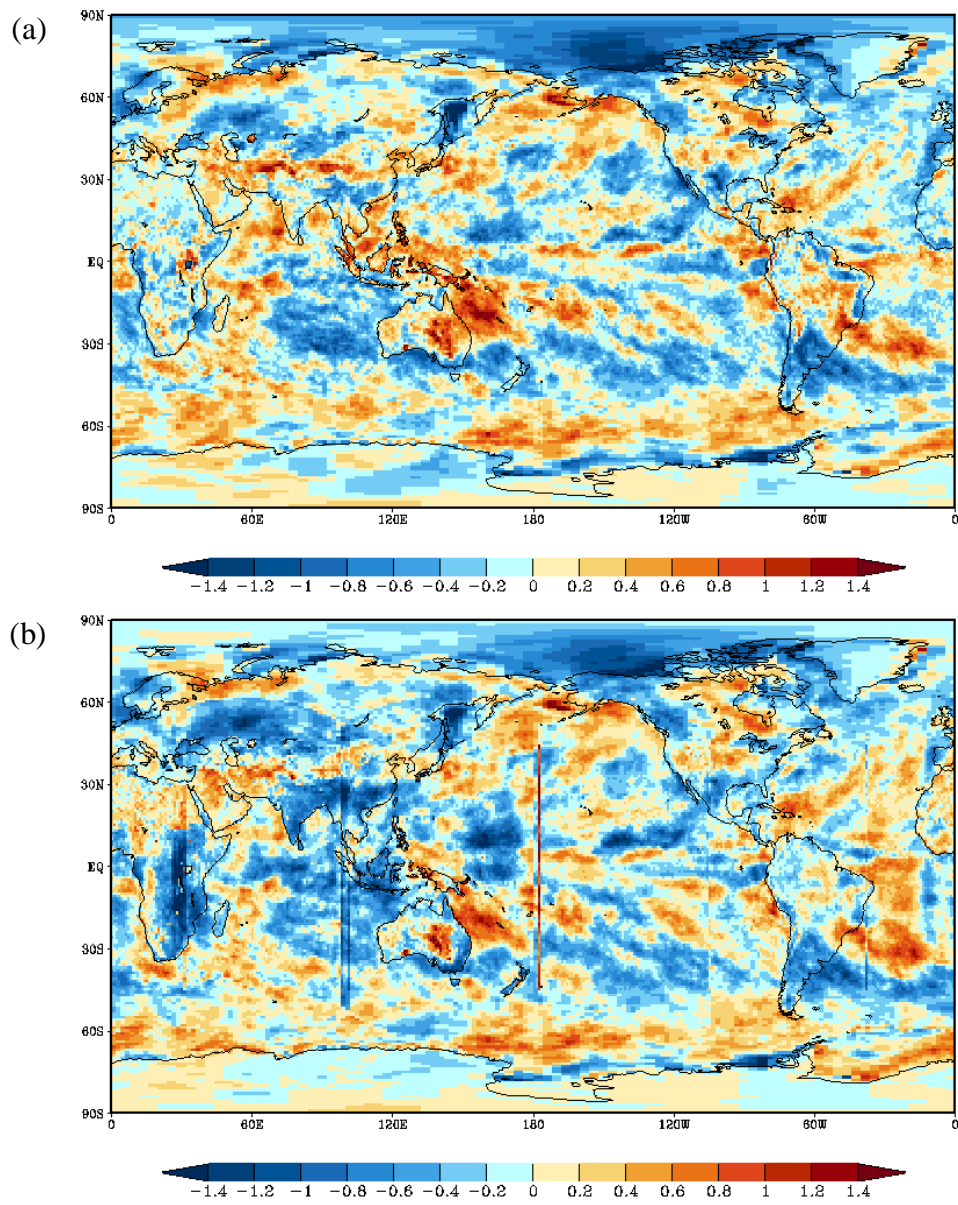


Figure 5 Regional trends ( $\text{Wm}^{-2}$  per decade) in SW TOA flux for March 2000-December 2010 from (a) EBAF Ed2.6r and (b) SYN1deg Ed2.6.



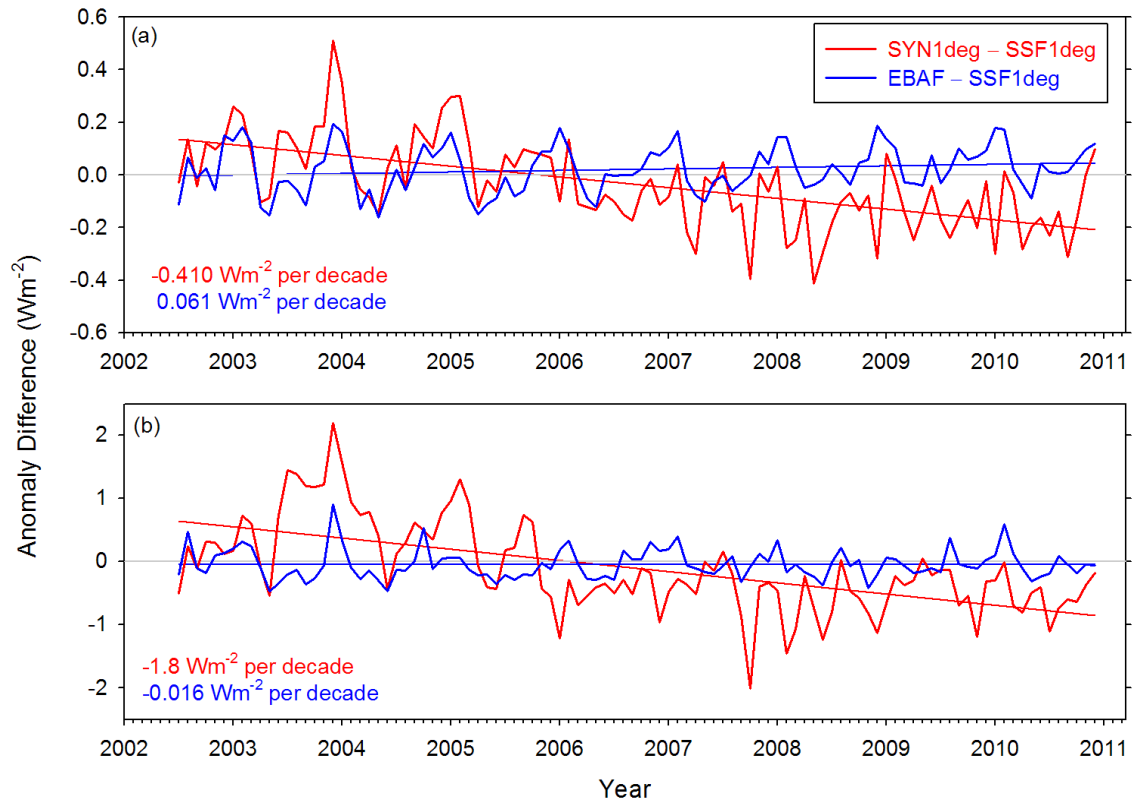


Figure 6 SW TOA flux anomaly difference between SYN1deg and SSF1deg Ed2.6r and between EBAF and SSF1deg Ed2.6r for (a) 60°S–60°N, and (b) the western sector of the region covered by GMS-5, GOES-9, and MTSAT-1R geostationary satellites (60°S–60°N, 101.5°E–140°E) for July 2002–December 2010. Straight lines correspond to least-square fits through the anomaly difference curves. Slopes are in units  $\text{Wm}^{-2}$  per decade.

## 5. Considerations for Model-Observation Comparisons

As noted in the previous section, the CERES monthly SW TOA fluxes account for diurnal cycle. Since the CERES instruments provide global coverage daily, monthly mean regional fluxes are based upon complete daily samples over the entire globe.

Users interested in utilizing CERES EBAF Ed2.6r to explore short-term trends in SW TOA flux are cautioned that CERES Terra observations are used for the period from March 2000-June 2002, while both CERES Terra and Aqua are used from July 2002 onwards. Consequently, there can be small artificial discontinuity in the data in July 2002 due to the introduction of Aqua.

When the solar zenith angle is greater than  $90^\circ$ , twilight flux (Kato and Loeb, 2003) is added to the outgoing SW flux in order to take into account the atmospheric refraction of light. The magnitude of this correction varies with latitude and season, and is determined independently for all-sky and clear-sky conditions. In general, the regional correction is less than  $0.5 \text{ W m}^{-2}$  and the global mean correction is  $0.2 \text{ W m}^{-2}$ . Due to the contribution of twilight, there are regions near the terminator in which outgoing SW TOA flux can exceed the incoming solar radiation. Users should be aware that in these cases, albedos (derived from the ratio of outgoing SW to incoming solar radiation) exceed unity.

Since TOA flux represents a flow of radiant energy per unit area, and varies with distance from the earth according to the inverse-square law, a reference level is also needed to define satellite-based TOA fluxes. From theoretical radiative transfer calculations using a model that accounts for spherical geometry, the optimal reference level for defining TOA fluxes in radiation budget studies for the earth is estimated to be approximately 20 km. At this reference level, there is no need to explicitly account for horizontal transmission of solar radiation through the atmosphere in the earth radiation budget calculation. In this context, therefore, the 20-km reference level corresponds to the effective radiative “top of atmosphere” for the planet. Since climate models generally use a plane-parallel model approximation to estimate TOA fluxes and the earth radiation budget, they implicitly assume zero horizontal transmission of solar radiation in the radiation budget equation, and do not need to specify a flux reference level. By defining satellite-based TOA flux estimates at a 20-km flux reference level, comparisons with plane-parallel climate model calculations are simplified since there is no need to explicitly correct plane-parallel climate model fluxes for horizontal transmission of solar radiation through a finite earth. For a more detailed discussion of reference level, please see Loeb et al. (2002).

## 6. Instrument Overview

See the first paragraph of Section 3 for an overview of the CERES instruments on the Terra and Aqua satellites.

## 7. References

The full version of CERES EBAF Ed2.6r is available from the following ordering site:

[http://ceres.larc.nasa.gov/order\\_data.php](http://ceres.larc.nasa.gov/order_data.php)

Doelling, D.R., N.G. Loeb, D.F. Keyes, M.L. Nordeen, D. Morstad, B.A. Wielicki, D.F. Young, and M. Sun, 2012: Geostationary enhanced temporal interpolation for CERES flux products. *J. Appl. Meteor. and Clim.* (submitted).

- Hansen, J. et al. Earth's energy imbalance: confirmation and implications. *Science* **308**, 1431–1435 (2005).
- Kato, S., and N. G. Loeb, 2003: Twilight irradiance reflected by the earth estimated from Clouds and the Earth's Radiant Energy System (CERES) measurements. *J. Climate*, **16**, 2646–2650.
- Kato, S., and N.G. Loeb, 2005: Top-of-atmosphere shortwave broadband observed radiance and estimated irradiance over polar regions from Clouds and the Earth's Radiant Energy System (CERES) instruments on Terra. *J. Geophys. Res.*, **110**, doi:10.1029/2004JD005308.
- Loeb, N. G., K. J. Priestley, D. P. Kratz, E. B. Geier, R. N. Green, B. A. Wielicki, P. O. R. Hinton, and S. K. Nolan, 2001: Determination of unfiltered radiances from the Clouds and the Earth's Radiant Energy System (CERES) instrument. *J. Appl. Meteor.*, **40**, 822–835.
- Loeb, N.G., N. M. Smith, S. Kato, W. F. Miller, S. K. Gupta, P. Minnis, and B. A. Wielicki, 2003: Angular distribution models for top-of-atmosphere radiative flux estimation from the Clouds and the Earth's Radiant Energy System instrument on the Tropical Rainfall Measuring Mission Satellite. Part I: Methodology. *J. Appl. Meteor.*, **42**, 240–265.
- Loeb, N.G., S. Kato, K. Loukachine, and N. M. Smith, 2005: Angular distribution models for top-of-atmosphere radiative flux estimation from the Clouds and the Earth's Radiant Energy System instrument on the Terra satellite. Part I: Methodology. *J. Atmos. Oceanic Technol.*, **22**, 338–351.
- Loeb, N. G., J. M. Lyman, G. C. Johnson, R. P. Allan, D. R. Doelling, T. Wong, B. J. Soden, and G. L. Stephens, 2012a: Observed changes in top-of-the-atmosphere radiation and upper-ocean heating consistent within uncertainty, *Nature Geosciences*, **5**(2), 110–113. doi:10.1038/ngeo1375.
- Loeb, N. G., S. Kato, W. Su, T. Wong, F. G. Rose, D. R. Doelling, and J. Norris, 2012b: Advances in understanding top-of-atmosphere radiation variability from satellite observations, *Surveys in Geophysics*, doi: 10.1007/s10712-012-9175-1.
- Loeb, N.G., S. Kato, K. Loukachine, and N. Manalo-Smith 2007, Angular distribution models for top-of-atmosphere radiative flux estimation from the Clouds and the Earth's Radiant Energy System instrument on the Terra satellite. Part II: Validation, *J. Atmos. Oceanic Technology*, **24**, 564–584.
- Loeb, N.G., W. Sun, W.F. Miller, K. Loukachine, and R. Davies, 2006: Fusion of CERES, MISR and MODIS measurements for top-of-atmosphere radiative flux validation, *J. Geophys. Res.*, **111**, D18209, doi:10.1029/2006JD007146.
- Loeb, N.G., B.A. Wielicki, D.R. Doelling, G.L. Smith, D.F. Keyes, S. Kato, N.M. Smith, and T. Wong, 2009: Towards optimal closure of the earth's top-of-atmosphere radiation budget. *J. Climate*, **22**, 748–766.
- Loeb, N.G., S. Kato, and B.A. Wielicki, 2002: Defining top-of-atmosphere flux reference level for Earth Radiation Budget studies, *J. Climate*, **15**, 3301–3309.
- Lyman, J.M., and G.C. Johnson, 2008: Estimating annual global upper-ocean heat content anomalies despite irregular in situ ocean sampling. *J. Clim.* **21**, 5629–5641.
- Minnis P., S. Sun-Mack, D.F. Young, P.W. Heck, D.P. Garber, Y. Chen, D.A. Spangenberg, R.F. Arduini, Q.Z. Trepte, W.L. Smith, Jr., J.K. Ayers, S.C. Gibson, W.F. Miller, V. Chakrapani, Y. Takano, K.-N. Liou, Y. Xie, 2011: CERES Edition-2 cloud property retrievals using

TRMM VIRS and Terra and Aqua MODIS data, Part I: Algorithms, IEEE Trans. Geosci. and Rem. Sens. (in press).

Purkey, S.G., and G.C. Johnson, 2010: Warming of global abyssal and deep southern ocean waters between the 1990s and 2000s: contributions to global heat and sea level rise budgets. *J. Clim* **23**, 6336–6351.

Roemmich, D. et al. Argo: the challenge of continuing 10 years of progress. *Oceanography* **22**, 46–55 (2009).

Thomas S., K.J. Priestley, N. Manalo-Smith, N.G. Loeb, P.C. Hess, M. Shankar, D.R. Walikainen, Z.P. Szewczyk, R.S. Wilson, D.L. Cooper, 2010: Characterization of the Clouds and the Earth's Radiant Energy System (CERES) sensors on the Terra and Aqua spacecraft, *Proc. SPIE, Earth Observing Systems XV*, Vol. 7807, 780702, August 2010.

Trenberth, K.E., 2009: An imperative for climate change planning: tracking Earth's global energy. *Current Opinion in Environmental Sustainability* **1**, 19–27.

## **8. Revision History**

[Document changes in the dataset and the technical note if a new version replaces an older version published on the ESG.]

Rev 0 – 08/09/2011- This is a new document/dataset

Rev 1 – 03/05/2012 – Updated to Edition2.6r. EBAF Ed2.6r corrects a code error in the calculation of global mean quantities in EBAF Ed2.6. Also updates temporal extent to 06/2011 from 12/2010. This version also updates some of the references.